Inorganic Chemistry

ARTICLE

pubs.acs.org/IC

Boron-Bridged π-Conjugated Ladders as Efficient Electron-Transporting Emitters

Di Li, Yang Yuan, Hai Bi, Dandan Yao, Xingjia Zhao, Wenjing Tian, Yue Wang, and Hongyu Zhang*

State Key Laboratory of Supramolecular Structure and Materials, College of Chemistry, Jilin University, Changchun 130012, People's Republic of China

Supporting Information

ABSTRACT: Four diboron-bridged ladder molecules **1**−**4** have been designed and synthesized. X-ray diffraction analysis revealed that the bulky phenyl substituents on boron centers efficiently prevented π stacking of the luminescent ladder unit. Characterizations of these complexes demonstrated that the construction of diboron-containing ladder-type skeletons endowed these materials with good thermal stability, high fluorescence quantum yields, and strong electron affinity. The highly efficient nondoped organic light-emitting diodes using complexes **1** and **2** as electron-transporting emitters exhibited maximum luminance values of 16 930 and 18 060 cd/m^2 with turn-on voltages of 3.5 and 2.5 V as well as maximum luminous efficiencies of 6.4 and 5.4 cd/A, respectively.

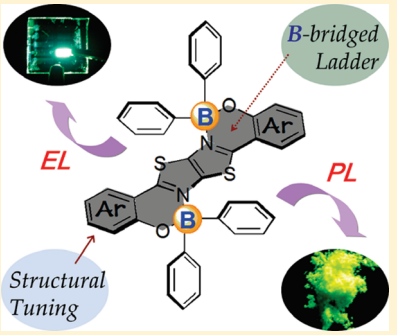

INTRODUCTION

Ladder-type π-conjugated molecules with fully ring-fused structures have attracted considerable attention in the field of organic electronics.[1] The flat and rigid π-conjugated skeletons of such molecules give rise to a set of desired properties such as intense luminescence, good thermal stability, and high carrier mobility that are important in terms of their applications in high-performance optoelectronics including organic light-emitting diodes (OLEDs), organic field effect transistors, and lasers.[2] To modulate the electronic structure of ladder-type molecules and obtain the required optical properties, various bridging atoms such as silicon, sulfur, selenium, phosphorus, boron, and nitrogen have been introduced to the π-conjugated skeleton.[3−9] Recently, multiboron-bridged ladder-type π-conjugated compounds reported by other groups and us have proved to be emissive organic solids with high electron affinity, which enables them to be used as both emitting and electron-transporting materials to fabricate structurally simple and high-performance electroluminescent (EL) devices.[10,11] In this kind of system, the incorporation of boryl groups into the π-conjugated skeleton allows intramolecular coordination from the Lewis basic nitrogen atom to the boron atom,[12−14] and the produced fully ring-fused structures not only constrain the π-conjugated framework to intensify the emission but also affect the electronic state by lowering the lowest unoccupied molecular orbital (LUMO) level to enhance the electron affinity. Although this type of molecule has promising potential in the fields of OLEDs, only a few ladder-type boron-containing systems have been achieved to date probably because of the lack of efficient synthetic routes. In this regard, constructing new ladder-type multiboron-doped π-conjugated skeletons by simple synthetic routes has become a very important issue that arouses our strong interest.

Recently, we have developed a simple approach to synthesize luminescent π-conjugated ladders bearing the boron element as bridges.[12] To continue our effort in the development of boron-containing ladder molecules with enhanced emission and electron-transporting properties, we herein report the synthesis and light-emitting properties of a series of novel diboron-bridged ladders. In the present work, we choose phenol-substituted thiazolothiazole derivatives as the key building units and incorporate two phenyl-substituted boron moieties into the backbones to construct a rigid extended π-conjugated skeleton (Chart 1). This type of precursor is selected because of its inherent electron-deficient character as well as its high reactivity with boron reagents by O−B−N chelation. This design aims at producing a novel ladder-type system with intense emission and high electron affinity to be used as both high-performance emitters and electron-transporting materials. Further functionalization of the system has been performed on the molecular structure by introducing electron-withdrawing/donating groups into the π-conjugated plane. The single-crystal X-ray structures, thermal stabilities, photophysical and electrochemical properties of these complexes have been investigated to study the characteristics of the π system and the impact of modification. Furthermore, the EL properties of this system are also presented to demonstrate their application potential in OLEDs.

Received: December 22, 2010
Published: May 10, 2011

Chart 1. Design Strategy toward a Diboron-Containing Ladder

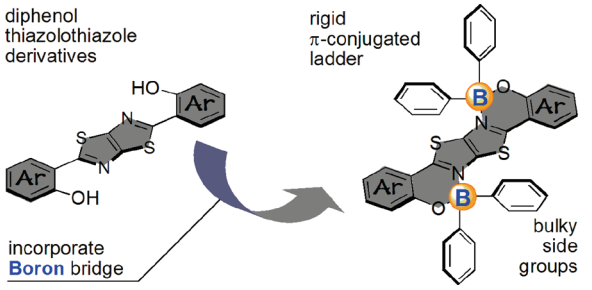

EXPERIMENTAL SECTION

General Procedure. All starting materials were purchased from Aldrich Chemical Co. and used without further purification. The solvents for the syntheses were freshly distilled over appropriate drying reagents. All experiments were performed under a nitrogen atmosphere using standard Schlenk techniques. ^{1}H NMR spectra were measured on a Bruker AVANCE 500 MHz spectrometer with tetramethylsilane as the internal standard. Mass spectra were recorded on a Shimadzu AXIMA-CFR MALDI-TOF mass spectrometer. Elemental analyses were performed on a flash EA 1112 spectrometer. Differential scanning calorimetry (DSC) measurements were performed on a Netzsch DSC204 instrument. Thermogravimetric analyses (TGA) were performed on a TA Q500 thermogravimeter. UV−vis absorption spectra were recorded using a Perkin-Elmer UV−vis Lambdazo spectrometer. The emission spectra were recorded using a Shimadzu RF-5301 PC spectrometer. Tris(8-hydroxyquinolino)aluminum (Alq_3) was purchased from Aldrich and purified by vacuum sublimation. *N*,*N*′-Di-1-naphthyl-*N*,*N*′-diphenyl-(1,1′-biphenyl)-4,4′-diamine (NPB),[15] 2,5-bis(2-hydroxyphenyl)thiazolo-[5,4-*d*]thiazole (**H_2L1**), 2,5-bis(2-hydroxy-5-fluorophenyl)thiazolo[5,4-*d*]-thiazole (**H_2L2**), 2,5-bis(2-hydroxy-5-methoxyphenyl)thiazolo[5,4-*d*]thiazole (**H_2L3**), and 2,5-bis(2-hydroxy-4-methoxyphenyl)thiazolo[5,4-*d*]thiazole (**H_2L4**) were synthesized according to the literature procedures.[16]

*$Ph_2B(\mu$-L1$)BPh_2$ (**1**).* To a rapidly stirred solution of **H_2L1** (200 mg, 0.55 mmol) in tetrahydrofuran (THF; 20 mL) was added BPh_3 (293 mg, 1.21 mmol) in THF (5 mL), and the solution was refluxed for 12 h. The volatiles were removed under vacuum, and the residual solid was purified by vacuum sublimation to give complex **1** as a yellow solid (180 mg, 50% yield). ^{1}H NMR ($CDCl_3$, ppm): δ 7.44 (t, J = 7.5 Hz, 2 H), 7.36−7.28 (m, 20 H), 7.17 (d, J = 7.5 Hz, 2 H), 7.14 (d, J = 7.5 Hz, 2 H), 6.78 (t, J = 7.5 Hz, 2 H). MS: m/z 653.1 $[M]^+$ (calcd m/z 654.2). Anal. Calcd for $C_{40}H_{28}B_2N_2O_2S_2$: C, 73.41; H, 4.31; N, 4.28; S, 9.80. Found: C, 73.35; H, 4.22; N, 4.28; S, 10.06.

*$Ph_2B(\mu$-L2$)BPh_2$ (**2**).* In the same manner as that described for **1**, the reaction of **H_2L2** (100 mg, 0.28 mmol) and BPh_3 (144 mg, 0.60 mmol) provided **2** as an orange-yellow solid (82 mg, 43% yield). ^{1}H NMR ($CDCl_3$, ppm): δ 7.33−7.29 (m, 20 H), 7.20−7.14 (m, 4 H), 6.81 (dd, J = 7.5 and 2.5 Hz, 2 H). MS: m/z 690.0 $[M]^+$ (calcd m/z 690.2). Anal. Calcd for $C_{40}H_{26}B_2F_2N_2O_2S_2$: C, 69.59; H, 3.80; N, 4.06; S, 9.29. Found: C, 69.55; H, 3.75; N, 4.07; S, 9.57.

*$Ph_2B(\mu$-L3$)BPh_2$ (**3**).* In the same manner as that described for **1**, the reaction of **H_2L3** (190 mg, 0.49 mmol) and BPh_3 (266 mg, 1.10 mmol) provided **3** as an orange solid (182 mg, 51% yield). ^{1}H NMR ($CDCl_3$, ppm): δ 7.36−7.28 (m, 20 H), 7.13 (d, J = 9 Hz, 2 H), 7.07 (dd, J = 9 and 2.5 Hz, 2 H), 6.51 (d, J = 3 Hz, 2 H), 3.71 (s, 6 H). MS: m/z 714.0 $[M]^+$ (calcd m/z 714.2). Anal. Calcd for $C_{42}H_{32}B_2N_2O_4S_2$: C, 70.61; H, 4.51; N, 3.92; S, 8.98. Found: C, 70.38; H, 4.45; N, 3.92; S, 9.23.

*$Ph_2B(\mu$-L4$)BPh_2$ (**4**).* In the same manner as that described for **1**, the reaction of **H_2L4** (190 mg, 0.49 mmol) and BPh_3 (266 mg, 1.10 mmol) provided **4** as a yellow solid (140 mg, 40% yield). ^{1}H NMR ($CDCl_3$, ppm): δ 7.35−7.28 (m, 20 H), 7.01 (d, J = 9 Hz, 2 H), 6.61 (d, J = 2.5 Hz, 2 H), 6.35 (dd, J = 9 and 2.5 Hz, 2 H), 3.82 (s, 6 H). MS: m/z 713.2 $[M]^+$ (calcd m/z 714.2). Anal. Calcd for $C_{42}H_{32}B_2N_2O_4S_2$: C, 70.61; H, 4.51; N, 3.92; S, 8.98. Found: C, 70.33; H, 4.42; N, 3.87; S, 8.88.

Scheme 1. Synthetic Procedure for Diboron Complexes 1−4

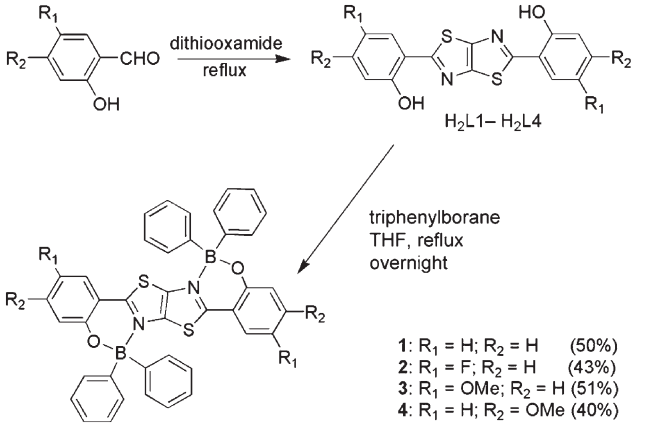

X-ray Diffraction. Diffraction data were collected on a Rigaku RAXIS-PRID diffractometer using the ω-scan mode with graphite-monochromator Mo Kα radiation. The structures were solved with direct methods using the *SHELXTL* programs[17] and refined with full-matrix least squares on F^2. Non-hydrogen atoms were refined anisotropically. The positions of the hydrogen atoms were calculated and refined isotropically.

Photoluminescent (PL) Quantum Yield Measurements. The solution fluorescence quantum yields were measured in dilute CH_2Cl_2 relative to quinine sulfate in an aqueous sulfuric acid solution (λ_{exc} = 365 nm; Φ_F = 0.546) at room temperature. The quantum yields were calculated using previously known procedures.[18] The solid-state quantum yields were measured using an integrating sphere with an excitation wavelength of 325 nm for all of the complexes.

Electrochemical Measurements. Cyclic voltammetry (CV) was performed using a BAS 100W instrument with a scan rate of 100 mV/s. A three-electrode configuration was used for the measurements: a platinum electrode as the working electrode, a platinum wire as the counter electrode, and an Ag/Ag^+ electrode as the reference electrode. A 0.1 M solution of tetrabutylammonium perchlorate (TBAP) in THF was used as the supporting electrolyte. The ferrocene/ferrocenium (Fc/Fc^+) couple was used as the internal standard.

Theoretical Calculations. The ground-state geometries were fully optimized by the density functional theory (DFT)[19] method with the Becke three-parameter hybrid exchange, the Lee−Yang−Parr correlation functional[20] (B3LYP), and the 6-31G* basis set using the *Gaussian 03* software package.[21]

Fabrication of EL Devices. Indium−tin oxide (ITO)-coated glass was used as the substrate. It was cleaned by sonication successively in a detergent solution, acetone, methanol, and deionized water before use. The devices were prepared in vacuum at a pressure of 5×10^{-6} Torr. Organic layers were deposited onto the substrate at a rate of 1−2 Å/s. After organic film deposition, LiF and aluminum were thermally evaporated onto the organic surface. The thicknesses of the organic materials and the cathode layers were controlled using a quartz crystal thickness monitor. The electrical characteristics of the devices were measured with a Keithley 2400 source meter. The EL spectra and luminance of the devices were obtained on a PR650 spectrometer.

RESULTS AND DISCUSSION

Syntheses. Scheme 1 shows the synthetic procedures for the diboron ladders **1**−**4**. Simple mixing of the ligands and boron

dx.doi.org/10.1021/ic102554j |*Inorg. Chem.* 2011, 50, 4825–4831

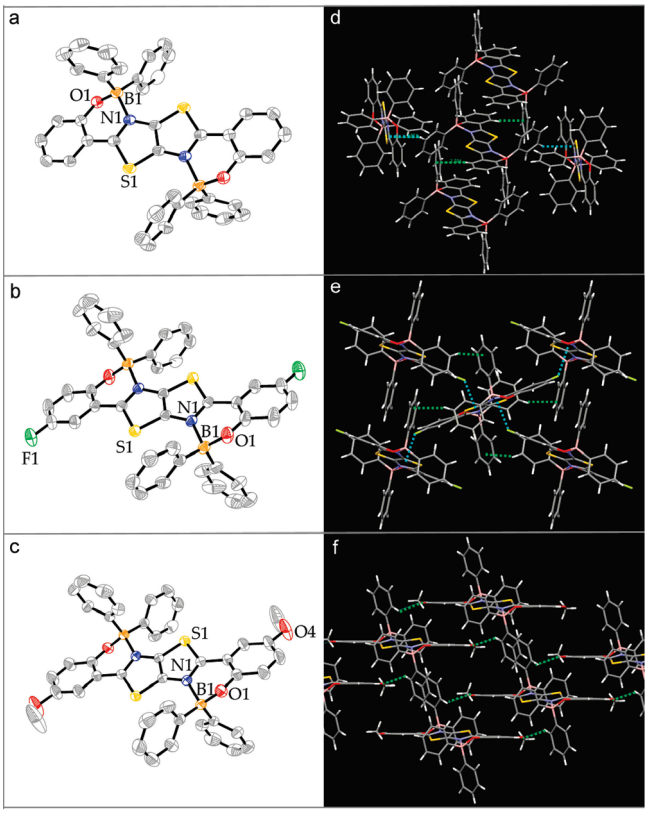

Figure 1. Molecular structures of complexes **1** (a), **2** (b), and **3** (c) with 50% thermal ellipsoids and packing structures of **1** (d), **2** (e), and **3** (f).

reagents in THF and subsequent purification by vacuum sublimation gave the targets **1**−**4** in moderate yields (40−51%), which were fully characterized by ^{1}H NMR spectroscopy, mass spectrometry (MS), element analyses, and/or X-ray crystal analysis. The skeletons were modified by introducing electron-withdrawing/donating groups into different sites of the backbones. The modification was performed during the syntheses of the relative ligands before boron chelation, and the ligands were obtained by condensation of dithiooxamide with the relative aromatic aldehydes at reflux temperature.

Crystal Structures. Single crystals of complexes **1**−**3** were obtained by vacuum sublimation, and their structures were determined by X-ray crystallography. The crystal lattices of **1**−**3** are all centrosymmetric, in which **1** and **2** belong to monoclinic space group $P2_1/c$ and **3** holds triclinic space group $P\bar{1}$. All boron atoms adopt a typical tetrahedral geometry to form N,O-chelate six-membered rings, which contribute to form the six-ring-fused ladder-type π-conjugated skeletons (Figure 1a−c). In the ladder-type skeleton of complex **1**, the six-membered rings constructed by boron chelation take a chair conformation in which the oxygen and boron atoms deviate from the central thiazolothiazole plane by 0.59 and 0.16 Å, respectively, in opposite directions. The bond lengths of B−N, B−O, and B−C are 1.658, 1.470, 1.608 Å, respectively, which are similar to those of the organoboron quinolates reported previously.[22] The dihedral angle between the central thiazolothiazole plane and the terminal phenylene plane is 14.53°, indicating that the ladder-type skeletons have certain distortions from the coplanar framework. Parts d−f of Figure 1 show the crystal packing structures of **1**−**3**. No significant interfacial π−π interactions are found for all of the complexes in their packing structures because of the large steric hindrance of peripheral phenyl rings. This structural feature should play an important role in reducing excimer formation in the solid state, as was already observed in ladder-type structures.[4c,23] In the packing structure of **1**, one molecule is connected with four adjacent molecules by two types of C−H···π intermolecular interactions: C−H(ladder)···π(Ph) (d = 2.70 Å; θ = 137.8°) and C−H(Ph)···π(ladder) (d = 2.87 Å; θ = 146.6°), as depicted in Figure 1d. Figure 1e shows the packing structure of **2**. Each molecule interacts with four adjacent molecules by C−F-(ladder)···π(ladder) (d = 2.89 Å; θ = 132.7°) interactions to form the molecular stacking, which is further stabilized by C−H(Ph)···π(Ph) (d = 2.81 Å; θ = 142.1°) interactions. In complex **3**, one-dimensional molecular columns are formed by C−H···O (d = 2.71 Å; θ = 140.6°) hydrogen-bonding interactions. These intermolecular interactions observed in the crystals **1**−**3** might be of benefit in terms of their charge carrier mobility.

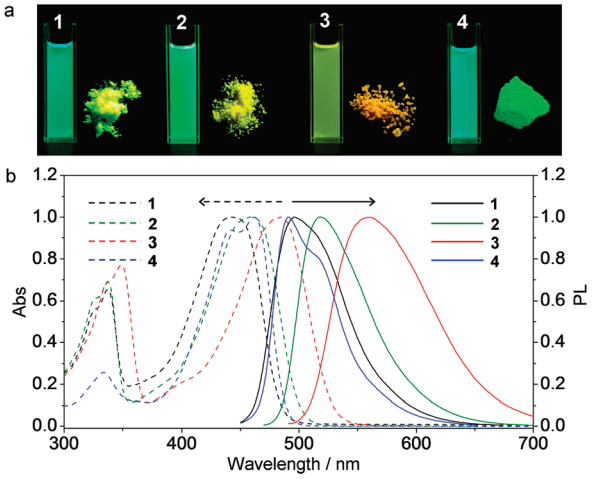

Figure 2. (a) Photographs in solution and the solid state under UV light (λ_{ex} = 365 nm) and (b) absorption and emission spectra of diboron complexes **1**−**4**.

Thermal Analyses. The thermal properties of **1**−**4** were characterized by TGA and DSC under a nitrogen atmosphere (Figures S9 and S10 in the Supporting Information). The melting points of **1**−**4** measured by DSC examinations are 332, 340, 405, and 352 °C, respectively. Complex **3** has the highest melting point among these boron species, which should be a result of intermolecular interactions of hydrogen bonds that condensed the molecular packing. Notably, complexes **1**−**4** had already partially decomposed before or during their melt in the DSC examinations because the measured melting points are close to their decomposition temperatures. As a result, the second cycles of the DSC measurements show no endo- or exothermic peaks; thus, the glass transition temperatures (T_g) of these complexes cannot be determined. The decomposition temperatures with a 5% weight loss (T_{dS}) of **1**−**4** are 346, 341, 378, and 374 °C, respectively. Methoxyl-substituted complexes **3** and **4** exhibit higher decomposition temperatures than those of **1** and **2**, probably owing to the intermolecular hydrogen bonds observed in the crystal structure. Thermal analyses indicate that the diboron-containing ladders **1**−**4** exhibit excellent thermal stability, which ensures that they are stable and suitable for vacuum evaporation in OLEDs.

dx.doi.org/10.1021/ic102554j |*Inorg. Chem.* 2011, 50, 4825–4831

Table 1. Photophysical Properties, Electrochemical Data, and Energy Levels of Complexes 1−4

		λ_{em} (nm)		Φ_F			experimental (eV)	
compd	λ_{abs} (nm)[a,b] (log ε)	solution[a]	powder	solution[a]	powder	$E_{red}^{1/2}$ (V)[c,d]	HOMO	LUMO
1	442 (4.45)	496	523	0.78	0.56	−1.75, *e*	−5.57[f]	−3.05
2	460 (4.44)	518	547	0.79	0.31	−1.58, −2.22	−5.68[f]	−3.22
3	481 (4.56)	561	563	0.38	0.12	−1.69, −2.26	−5.45[f]	−3.11
4	460 (4.54)	491	517	0.82	0.15	−1.92, −2.43	−5.41[f]	−2.88

[a] Data were collected in CH_2Cl_2 (1×10^{-4} M). [b] Only the longest absorption maxima are shown. [c] Potentials are given versus Fc/Fc^+. [d] Measured in THF. [e] Not observed. [f] Calculated from the optical band gap and the LUMO energy.

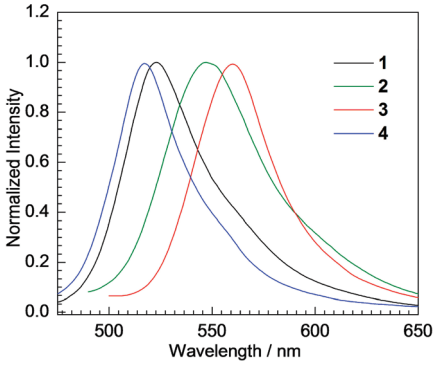

Figure 3. Solid-state emission spectra of diboron complexes **1**−**4**.

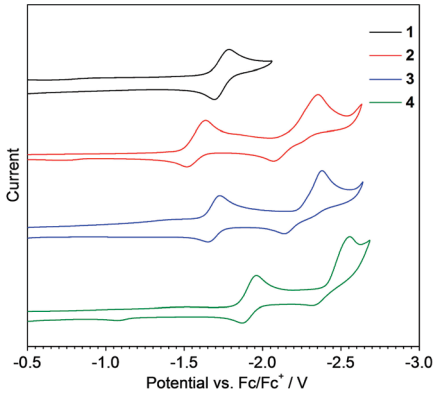

Figure 4. Cyclic voltammograms of **1**−**4** in THF (1 mM), measured with TBAP (0.1 M) as the supporting electrolyte at a scan rate of 100 mV/s.

Photophysical Properties. All of the boron complexes are highly emissive in both solution and the solid state, as shown in Figure 2a. The UV−vis absorption and fluorescence spectra of **1**−**4** in CH_2Cl_2 are shown in Figure 2b, and the data are summarized in Table 1.

The absorption spectrum of **2** is red-shifted by 18 nm compared to **1**. Interestingly, compared with complex **1**, the absorption maximum of **3** with the electron-donating methoxyl groups on the para position of the oxygen atoms is red-shifted by about 39 nm, while that of **4** with the methoxyl groups on the meta position of the oxygen atoms is only red-shifted by about 18 nm. This observation reflects that the substituted sites significantly affect the electronic structure of this type of ladder skeleton.

In the fluorescence spectra, complexes **1**−**4** show intense green or yellow fluorescence with the maximum wavelengths at 496, 518, 561, and 491 nm, respectively. Compared with complex **1**, the emission maxima of **2** and **3** are red-shifted by 22 and 65 nm, respectively, consistent with the trend observed in the absorption maxima. The emission spectrum of complex **4** is slightly blue-shifted by 5 nm compared to that of **1**. Alkoxylation of the ladder skeleton on different positions produces obviously different optical properties, probably because of their different effects on the electronic structures. For complex **3**, alkoxylation on the para position of the oxygen atoms effectively pushes the highest occupied molecular orbital (HOMO) level up, thus narrowing the energy gap, while for complex **4**, alkoxylation on the meta position of the oxygen atoms increases both HOMO and LUMO levels by a similar extent. Notably, the fluorescence quantum yields for **1**, **2**, and **4** are all around 0.80 in CH_2Cl_2, which are much higher than most reported ladder-type boron-doped species.[24] The solid-state fluorescence has also been investigated, as shown in Figure 3. Interestingly, the fluorescences of **2** and **3** are red-shifted by 24 and 40 nm, respectively, compared to that of **1**, and the emission band of **4** is blue-shifted by about 6 nm compared to that of **1**, reflecting that the molecular packing also greatly affects their optical properties. Moreover, the emission spectra of complexes **1**, **2**, and **4** in the solid state are red-shifted compared to those of solutions, which can be attributed to the C−F···π and/or C−H···π intermolecular interactions, as demonstrated by the crystal structures. The solid-state fluorescence quantum yields of these ladders are also remarkable in the reported π-conjugated molecules, especially for that of **1**, with the value reaching 0.56. Complex **1** exhibits relatively high quantum yield both in solution and in the solid state, which is probably due to the fact that the absence of fluoro or methoxyl substituents on the ladder increases the molecular rigidity and weakens the intermolecular interactions. Actually, although the π systems have extended ladder-type frameworks, the bulky phenyl groups attached to the boron centers prevent efficient π stacking in their aggregated state, which was also demonstrated by the X-ray structure analysis. This feature allows some of the complexes to maintain high fluorescence quantum yields in the solid state and enables them to be further used as emitting materials.

Electrochemical Properties. The electrochemical properties of **1**−**4** were characterized by CV, their cyclic voltammograms are shown in Figure 4, and the data are summarized in Table 1. All of the complexes **1**−**4** display reversible reduction peaks in the CV diagrams. Two sequential reduction peaks are observed for **2**−**4**; the first one is reversible, while the second one is quasi-reversible with a more negative value. In contrast, complex **1** only displays one reversible reduction wave. For **1**−**4**, the first half-wave potentials ($E_{red}^{1/2}$) attributed to the reduction of the

dx.doi.org/10.1021/ic102554j |*Inorg. Chem.* 2011, 50, 4825–4831

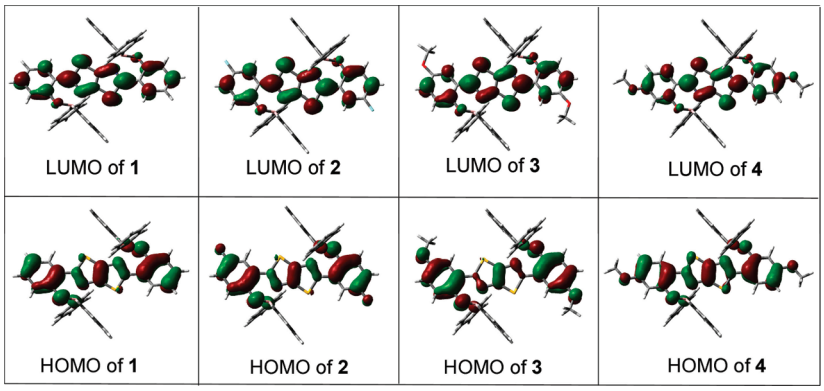

Figure 5. Molecular orbital diagrams for HOMOs and LUMOs of complexes **1**−**4**.

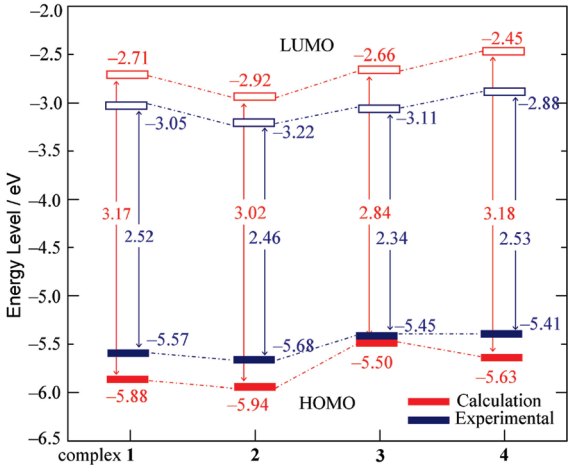

Figure 6. Calculated and experimental energy levels of diboron complexes **1**−**4**.

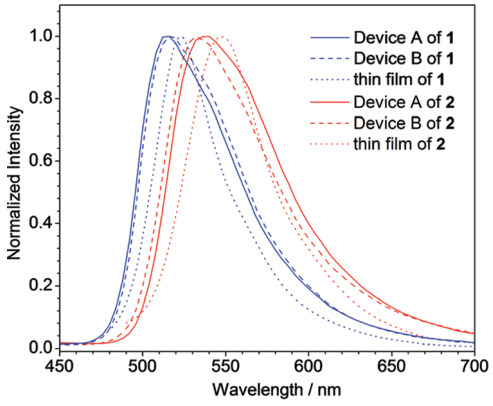

Figure 7. EL spectra of devices A and B and fluorescent spectra of thin films based on complexes **1** and **2**.

π-conjugated ladder are located from −1.58 to −1.92 V (vs Fc/Fc^+), in which slight shifts are observed owing to the effect of modification. These values are similar to those of the diboron-doped ladder-type molecules reported before, illustrating that the low LUMO levels of the π system are contributed by boron chelation, which makes the cathodic reductions easier and endows the complexes with high electron affinity. Notably, the first reduction potentials of **1**−**4** are less negative than that of Alq_3 (E_{pc} = −2.3 V),[25] one of the most widely used electron-transporting materials, which might be indicative of the good electron-transporting properties of these complexes in EL devices. On the basis of the reduction potentials, the LUMO energy levels are calculated and summarized in Table 1. Because we are unable to observe any oxidation within the electrochemical window of CH_2Cl_2 for **1**−**4**, their HOMO levels are empirically calculated from their LUMO energy levels and optical data (absorption edges in UV−vis spectra).

Molecular Orbital Calculations. DFT calculations were performed for complexes **1**−**4** to further understand the electronic structures and energy levels of these ladders. The plots and data of HOMOs and LUMOs are shown in Figures 5 and 6. The HOMOs and LOMOs of all of these complexes are mainly composed of π and π^* orbitals of the whole ligand, respectively, while the boryl moieties give little contribution. Compared with **1**, the electron-withdrawing effect of the fluorine atoms decreases the HOMO and LUMO levels in **2**, while the HOMO and LUMO levels are raised because of the electron-donating effect of the methoxyl groups in **3** and **4**. Moreover, different substituted sites also influence the energy levels. The LUMOs are partly donated on the substituted groups of **4** instead of **2** and **3**, just because of the different substituted positions of the introduced moieties on the main skeleton. The degree of variation for HOMOs/LUMOs and the band gaps of **1**−**4** are greatly influenced by the electronic properties and substituted sites of the introduced groups. The general trend of the calculated HOMO/LUMO levels and energy gaps agrees with the experimentally observed trend. The discrepancies of the HOMO/LUMO levels between calculated and experimental values can be attributed to the limitation of the ground-state DFT calculations.

EL Properties. Considering that complexes **1** and **2** have relatively high solid-state fluorescence quantum yields among the synthesized diboron ladders, we devote our major effort to studying the EL properties of **1** and **2**. Two types of devices were designed and fabricated to evaluate the electron-transport property and the electroluminescence of each complex. The first one was a four-layer device with the configuration of [ITO/NPB (15 nm)/BA (30 nm)/**1** or **2** (40 nm)/Alq_3 (15 nm)/LiF (0.5 nm)/Al (200 nm)] (device A). In device A, NPB was used as the hole-transport material, BA (Figure S11 in the Supporting Information) served as an additional hole buffer layer for the purpose of hindering the formation of exciplex between NPB and the boron complex, Alq_3 acted as an electron-transport layer, and

dx.doi.org/10.1021/ic102554j |*Inorg. Chem.* 2011, 50, 4825–4831

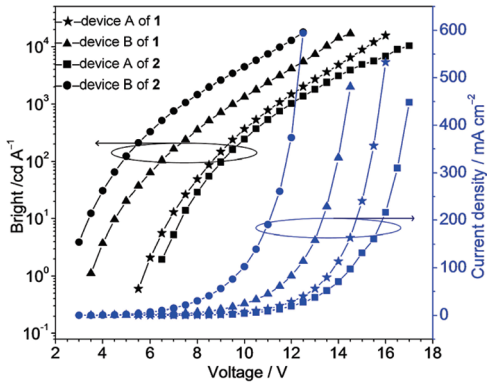

Figure 8. Current density−brightness−voltage characteristics of device A of complex **1** (★), device B of complex **1** (▲), device A of complex **2** (■), and device B of complex **2** (●).

complexes **1** or **2** acted as the emitting material. For complex **1**, this device was turned on at 5.5 V and produced a green color centered at 516 nm (Figure 7). Figure 8 shows the $J-V$ and $L-V$ characteristics of device A. It could reach a maximum brightness of 15 620 cd/m^2 at 16 V, a maximum luminous efficiency of 7.2 cd/A at 8.5 V, and a maximum power efficiency of 3.2 lm/W at 6 V. For complex **2**, device A was turned on at 6.5 V with the electroluminescence center at 532 nm and reached a maximum brightness of 10 340 cd/m^2 at 17 V, a maximum luminous efficiency of 6.3 cd/A at 9.5 V, and a maximum power efficiency of 2.1 lm/W at 6.5 V. Another kind of device with the configuration of [ITO/NPB (15 nm)/BA (30 nm)/**1** or **2** (55 nm)/LiF (0.5 nm)/Al (200 nm)] (device B) was also fabricated. With omission of the Alq_3 layer, here complexes **1** or **2** served as both the light-emitting layer and the electron-transport layer. Interestingly, the EL performance of device B, with a turn-on voltage of 3.5 V, a maximum brightness of 16 930 cd/m^2, and a maximum luminous efficiency of 6.4 cd/A at 5 V for **1** and a turn-on voltage of 2.5 V, a maximum brightness of 18 060 cd/m^2, and a maximum luminous efficiency of 5.4 cd/A at 5 V for **2**, showed a notable improvement. Device B with **2** as the emitter exhibits lower turn-on voltage and higher maximum brightness compared to that with **1** as the emitter. The power efficiencies of device B were 5.1 lm/W for **1** and 4.5 lm/W for **2**, which are greatly improved compared to those of device A (3.2 lm/W for **1** and 2.1 lm/W for **2**). This comparison clearly suggests that this kind of boron complex is an efficient emitter with excellent electron-transporting character. The EL spectra of devices A and B of each complex were nearly the same, and they matched well with the solid-state PL spectrum of the complex, as shown in Figure 7, demonstrating that the EL luminescence originated from the intrinsic emission of the complexes. We have not yet studied the lifetime of the devices, but the unencapsulated devices were stable and the emission color as well as $I-L-V$ did not change during measurement of the EL data in air. It is noteworthy that the EL performance of complexes **1** and **2** is at a high level in comparison with those previously reported for boron-doped ladders,[11,26] and the brightness and efficiency of devices A and B are much higher than those of the reported EL devices fabricated using other boron-containing emitter materials.

Electron Mobility. To further affirm the electron-transport ability, time-of-flight (TOF) carrier-mobility measurement based on complexes **1** and **2** with a device configuration of

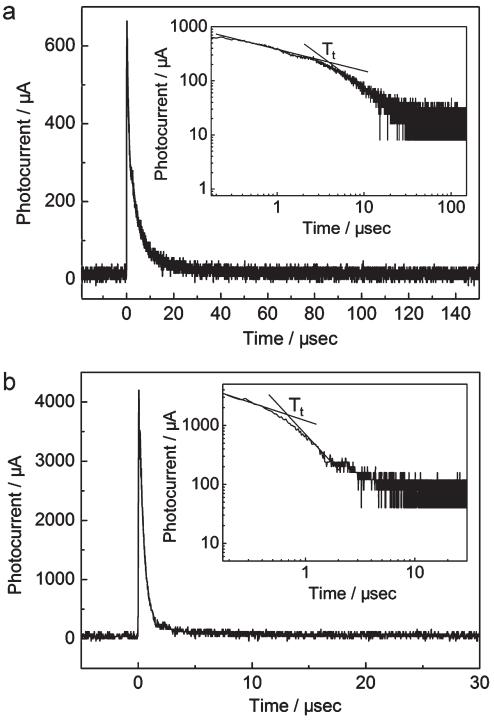

Figure 9. TOF transients for electrons at room temperature: (a) complex **1**, D = 1.95 μm, E = 1.54 × 10^5 V/cm, and T_t = 4.0 μs; (b) complex **2**, D = 1.18 μm, E = 2.12 × 10^5 V/cm, and T_t = 0.67 μs. Insets: Double-logarithmic plots of data in parts a and b.

ITO/complexes **1** or **2** (1−2 μm)/Al was carried out at room temperature. Figure 9 displays typical TOF transients of electrons for complexes **1** and **2** under an applied field. The transient photocurrent signals were dispersive, suggesting the presence of electron traps. According to the equation $\mu = D/ETt$, where D is the thickness of the transporting layer and E is the electrical field strength, the electron mobilities of the complexes on their vacuum-deposited films were determined to be 3.2 × 10^{-4} cm^2/V·s for complex **1** and 8.3 × 10^{-4} cm^2/V·s for complex **2**, which respectively are 30 and 80 times higher than that of the commonly used electron-transporting material Alq_3 (μ_e = 1 × 10^{-5} cm^2/V·s measured by means of the TOF method).[27]

CONCLUSION

In this study, we have designed and synthesized four novel diboron-containing π-conjugated ladders **1**−**4**. The system was prepared by a simple synthetic procedure, and further functionalization was easily realized by introducing electron-withdrawing/donating groups into different positions of the ladder skeleton. Single-crystal structures determined by X-ray diffraction analysis demonstrate that bulky aryl substituents on the boron centers prevent efficient π stacking. Characterizations of these complexes demonstrate that the construction of diboron-containing ladder-type skeletons endows these materials with good thermal stability, high fluorescence quantum yields, and strong electron affinity. Simple EL devices fabricated using complexes **1** and **2** as both emitter and electron-transporting materials exhibit the highest brightness and efficiency among boron-containing materials reported so far.

dx.doi.org/10.1021/ic102554j |*Inorg. Chem.* 2011, 50, 4825–4831

■ ASSOCIATED CONTENT

Supporting Information. Synthesis and characterization of the starting materials, ^{1}H NMR spectra, TGA and DSC curves of **1**−**4**, as well as crystallographic data for **1**−**3**, X-ray crystallographic data for **1**−**3** in CIF format, and Cartesian coordinates of **1**−**4** at the S_0-optimized geometry. This material is available free of charge via the Internet at http://pubs.acs.org.

■ AUTHOR INFORMATION

Corresponding Author
*E-mail: hongyuzhang@jlu.edu.cn.

■ ACKNOWLEDGMENT

This work was supported by the National Natural Science Foundation of China (Grants 50903037, 20921003, and 50733002) and the Major State Basic Research Development Program (Grant 2009CB623600).

■ REFERENCES

(1) (a) Kawaguchi, K.; Nozaki, K. *J. Org. Chem.* **2007**, *72*, 5119. (b) Sonntag, M.; Strohriegl, P. *Tetrahedron* **2006**, *62*, 8103. (c) Xiao, K.; Liu, Y.; Zhang, W.; Wang, F.; Gao, J.; Qin, J.; Hu, W.; Zhu, D. *J. Am. Chem. Soc.* **2005**, *127*, 3281. (d) Laquindanum, J. G.; Katz, H. E.; Lovinger, A. *J. Am. Chem. Soc.* **1998**, *120*, 664.

(2) (a) Craft, A.; Grimsdale, A. C.; Holmes, A. B. *Angew. Chem., Int. Ed.* **1998**, *37*, 402. (b) Watson, M. D.; Fechtenkötter, A.; Müllen, K. *Chem. Rev.* **2001**, *101*, 1267. (c) Anthony, J. E. *Angew. Chem., Int. Ed.* **2008**, *47*, 452.

(3) (a) Yamaguchi, S.; Xu, C.; Tamao, K. *J. Am. Chem. Soc.* **2003**, *125*, 13662. (b) Xu, C.; Wakamiya, A.; Yamaguchi, S. *J. Am. Chem. Soc.* **2005**, *127*, 1638. (c) Xu, C.; Wakamiya, A.; Yamaguchi, S. *Org. Lett.* **2004**, *6*, 3707. (d) Mouri, K.; Wakamiya, A.; Yamada, H.; Kajiwara, T.; Yamaguchi, S. *Org. Lett.* **2007**, *9*, 93.

(4) (a) Okamoto, T.; Kudoh, K.; Wakamiya, A.; Yamaguchi, S. *Chem.—Eur. J.* **2007**, *13*, 548. (b) Takimiya, K.; Kunugi, Y.; Konda, Y.; Ebata, H.; Toyoshima, Y.; Otsubo, T. *J. Am. Chem. Soc.* **2006**, *128*, 3044. (c) Wong, K.-T.; Chao, T.-C.; Chi, L.-C.; Chu, Y.-Y.; Balaiah, A.; Chiu, S.-F.; Liu, Y.-H.; Wang, Y. *Org. Lett.* **2006**, *8*, 5033. (d) Takimiya, K.; Ebata, H.; Sakamoto, K.; Izawa, T.; Otsubo, T.; Kunugi, Y. *J. Am. Chem. Soc.* **2006**, *128*, 12604. (e) Yamamoto, T.; Takimiya, K. *J. Am. Chem. Soc.* **2007**, *129*, 2224.

(5) (a) Fukazawa, A.; Hara, M.; Okamoto, T.; Son, E.-C.; Xu, C.; Tamao, K.; Yamaguchi, S. *Org. Lett.* **2008**, *10*, 913. (b) Fukazawa, A.; Yamada, H.; Yamaguchi, S. *Angew. Chem., Int. Ed.* **2008**, *47*, 5582.

(6) (a) Agou, T.; Kobayashi, J.; Kawashima, T. *Chem. Commun.* **2007**, 3204. (b) Agou, T.; Kobayashi, J.; Kawashima, T. *Org. Lett.* **2006**, *8*, 2241. (c) Agou, T.; Kobayashi, J.; Kawashima, T. *Chem.—Eur. J.* **2007**, *13*, 8051. (d) Agou, T.; Kobayashi, J.; Kawashima, T. *Org. Lett.* **2005**, *7*, 4373.

(7) (a) Bouchard, J.; Wakim, S.; Leclerc, M. *J. Org. Chem.* **2004**, *69*, 5705. (b) Patil, S. A.; Scherf, U.; Kadashchuk, A. *Adv. Funct. Mater.* **2003**, *13*, 609. (c) Wakim, S.; Bouchard, J.; Blouin, N.; Michaud, A.; Leclerc, M. *Org. Lett.* **2004**, *6*, 3413. (d) Kaszynski, P.; Dougherty, D. A. *J. Org. Chem.* **1993**, *58*, 5209.

(8) (a) Fukazawa, A.; Yamaguchi, S. *Chem.—Asian J.* **2009**, *4*, 1386. (b) Yamaguchi, S.; Wakamiya, A. *Pure Appl. Chem.* **2006**, *78*, 1413. (c) Zhao, C.-H.; Sakuda, E.; Wakamiya, A.; Yamaguchi, S. *Chem.—Eur. J.* **2009**, *15*, 10603.

(9) (a) Entwistle, C. D.; Marder, T. B. *Angew. Chem., Int. Ed.* **2002**, *41*, 2927. (b) Liu, Z.; Marder, T. B. *Angew. Chem., Int. Ed.* **2008**, *47*, 242.

(10) Zhao, Q.; Zhang, H.; Wakamiya, A.; Yamaguchi, S. *Synthesis* **2009**, 127.

(11) Zhang, Z. L.; Bi, H.; Zhang, Y.; Yao, D. D.; Gao, H. Z.; Fan, Y.; Zhang, H. Y.; Wang, Y.; Wang, Y. P.; Chen, Z. Y.; Ma, D. G. *Inorg. Chem.* **2009**, *48*, 7230.

(12) Li, D.; Zhang, Z.; Zhao, S.; Wang, Y.; Zhang, H. *Dalton Trans.* **2011**, *40*, 1279.

(13) (a) Liu, S. F.; Wu, Q.; Schmider, H. L.; Aziz, H.; Hu, N.-X.; Popović, Z.; Wang, S. *J. Am. Chem. Soc.* **2000**, *122*, 3671. (b) Rao, Y. L.; Amarne, H. S.; Zhao, B.; McCormick, T. M.; Martić, S.; Sun, Y.; Wang, R. Y.; Wang, S. *J. Am. Chem. Soc.* **2008**, *130*, 12898. (c) Baik, C.; Hudson, Z. M.; Amarne, H.; Wang, S. *J. Am. Chem. Soc.* **2009**, *131*, 14549. (d) Cui, Y.; Liu, Q.-D.; Bai, D.-R.; Jia, W.-L.; Tao, Y.; Wang, S. *Inorg. Chem.* **2005**, *44*, 601.

(14) (a) Qin, Y.; Kiburu, I.; Shah, S.; Jäkle, F. *Macromolecules* **2006**, *39*, 9041. (b) Qin, Y.; Kiburu, I.; Shah, S.; Jäkle, F. *Org. Lett.* **2006**, *8*, 5227. (c) Qin, Y.; Pagba, C.; Piotrowiak, P.; Jäkle, F. *J. Am. Chem. Soc.* **2004**, *126*, 7015. (d) Cheng, F.; Jäkle, F. *Chem. Commun.* **2010**, *46*, 3717.

(15) Koene, B. E.; Loy, D. E.; Thompson, M. E. *Chem. Mater.* **1998**, *10*, 2235.

(16) Johnson, J. R.; Ketcham, R. *J. Am. Chem. Soc.* **1960**, *82*, 2719.

(17) (a) *SHELXTL*, version 5.1; Siemens Industrial Automation, Inc.: Madison, WI, 1997. (b) Sheldrick, G. M. *SHELXS-97, Program for Crystal Structure Solution*; University of Göttingen: Göttingen, Germany, 1997.

(18) Ye, K.; Wang, J.; Sun, H.; Liu, Y.; Mu, Z.; Li, F.; Jiang, S.; Zhang, J.; Zhang, H.; Wang, Y.; Che, C. M. *J. Phys. Chem. B* **2004**, *109*, 8008.

(19) Runge, E.; Gross, E. K. U. *Phys. Rev. Lett.* **1984**, *52*, 997.

(20) Becke, A. D. *J. Chem. Phys.* **1993**, *98*, 5648.

(21) Frisch, M. J.; Trucks, G. W.; Schlegel, H. B.; Scuseria, G. E.; Robb, M. A.; Cheeseman, J. R.; Montgomery, J. A., Jr.; Vreven, T.; Kudin, K. N.; Burant, J. C.; Millam, J. M.; Iyengar, S. S.; Tomasi, J.; Barone, V.; Mennucci, B.; Cossi, M.; Scalmani, G.; Rega, N.; Petersson, G. A.; Nakatsuji, H.; Hada, M.; Ehara, M.; Toyota, K.; Fukuda, R.; Hasegawa, J.; Ishida, M.; Nakajima, T.; Honda, Y.; Kitao, O.; Nakai, H.; Klene, M.; Li, X.; Knox, J. E.; Hratchian, H. P.; Cross, J. B.; Adamo, C.; Jaramillo, J.; Gomperts, R.; Stratmann, R. E.; Yazyev, O.; Austin, A. J.; Cammi, R.; Pomelli, C.; Ochterski, J. W.; Ayala, P. Y.; Morokuma, K.; Voth, G. A.; Salvador, P.; Dannenberg, J. J.; Zakrzewski, V. G.; Dapprich, S.; Daniels, A. D.; Strain, M. C.; Farkas, O.; Malick, D. K.; Rabuck, A. D.; Raghavachari, K.; Foresman, J. B.; Ortiz, J. V.; Cui, Q.; Baboul, A. G.; Clifford, S.; Cioslowski, J.; Stefanov, B. B.; Liu, G.; Liashenko, A.; Piskorz, P.; Komaromi, I.; Martin, R. L.; Fox, D. J.; Keith, T.; Al-Laham, M. A.; Peng, C. Y.; Nanayakkara, A.; Challacombe, M.; Gill, P. M. W.; Johnson, B.; Chen, W.; Wong, M. W.; Gonzalez, C.; Pople, J. A. *Gaussian 03*, revision C.02; Gaussian, Inc.: Pittsburgh, PA, 2003.

(22) Wu, Q.; Esteghamatian, M.; Hu, N.-X.; Popovic, Z.; Enright, G.; Tao, Y.; Diorio, M.; Wang, S. *Chem. Mater.* **2000**, *12*, 79.

(23) Wong, K.-T.; Chi, L.-C.; Huang, S.-C.; Liao, Y.-L.; Liu, Y.-H.; Wang, Y. *Org. Lett.* **2006**, *8*, 5029.

(24) Cui, Y.; Wang, S. *J. Org. Chem.* **2006**, *71*, 6485.

(25) Shinar, J. *Organic light-emitting devices: a survey*; Springer-Verlag: New York, 2003.

(26) (a) Li, Y.; Liu, Y.; Bu, W.; Guo, J.; Wang, Y. *Chem. Commun.* **2000**, 1551. (b) Feng, J.; Li, F.; Gao, W. B.; Liu, S. Y.; Liu, Y.; Wang, Y. *Appl. Phys. Lett.* **2001**, *78*, 3479. (c) Liu, Y.; Guo, J.; Zhang, H.; Wang, Y. *Angew. Chem., Int. Ed.* **2002**, *41*, 182. (d) Zhang, H.; Huo, C.; Ye, K.; Zhang, P.; Tian, W.; Wang, Y. *Inorg. Chem.* **2006**, *45*, 2788. (e) Zhang, H.; Huo, C.; Zhang, J.; Zhang, P.; Tian, W.; Wang, Y. *Chem. Commun.* **2006**, 281.

(27) Barth, S.; Müller, P.; Riel, H.; Seidler, P. F.; Riess, W.; Vestweber, H.; Bässler, H. *J. Appl. Phys.* **2001**, *89*, 3711.